

Available online at [www.sciencedirect.com](http://www.sciencedirect.com)**ScienceDirect**

Procedia Manufacturing 29 (2019) 450–457

**Procedia**  
MANUFACTURING[www.elsevier.com/locate/procedia](http://www.elsevier.com/locate/procedia)

18th International Conference on Sheet Metal, SHEMET 2019

# Stress-state dependent fracture characterisation and modelling of an AZ31 magnesium sheet alloy at elevated temperatures

Bernd-Arno Behrens, Alexander Chugreev, Matthäus Dykiert\*

*Institute of Forming Technology and Machines (IFUM), Leibniz Universität Hannover  
An der Universität 2, 30823 Garbsen, Germany*

---

## Abstract

Due to a high specific strength, magnesium alloys have a high potential to be considered for lightweight solutions in automotive industry. For the numerical design of forming processes, it is important to describe the yielding as well as the fracture behaviour of a material as precisely as possible. In order to fully characterise the fracture behaviour of an AZ31 magnesium sheet alloy at elevated temperatures, a heated test setup for uniaxial tensile machines was developed. The setup allows an adjustment of the load application angle whereby a stress variation is achieved in the centre of the specimen. In order to determine the fracture strain for different temperatures and for varying stress states, a shear stress specimen (also known as butterfly specimen) was considered to perform mechanical experiments by means of this setup. Using numerical simulations, the specific stress development and strain value in the fracture zone, which is needed to calibrate stress state fracture models, was determined for each loading angle and temperature. For this purpose, an orthotropic yield criterion CPB06, which is suitable for depiction of the particular flow behaviour of magnesium alloys (e. g. compression-tension asymmetry), was used. By this means, sufficient data for the calibration of common stress state based fracture models could be provided and the MMC- (Modified Mohr-Coulomb) fracture model was parameterised.

© 2019 The Authors. Published by Elsevier B.V.

This is an open access article under the CC BY-NC-ND license (<https://creativecommons.org/licenses/by-nc-nd/4.0/>)

Selection and peer-review under responsibility of the organizing committee of SHEMET 2019.

*Keywords:* Magnesium sheet alloy AZ31; Fracture characterisation; Modified Mohr-Coulomb, Butterfly specimen

---

---

\* Corresponding author. Tel.: +49-511-762-3825; fax: +49-511-762-3007.

E-mail address: [dykiert@ifum.uni-hannover.de](mailto:dykiert@ifum.uni-hannover.de)

## 1. Introduction

Magnesium, as the lightest construction material, offers excellent properties such as low density, high specific strength and recyclability. For this reason, the demand for magnesium alloys in industries such as automotive and transportation is increasing steadily. For some time now, magnesium materials are used in casting applications. Due to cost-effective manufacturing processes like strip-casting, also a more widespread use of magnesium sheet alloys in sheet metal forming processes is likely. Nowadays, numerical approaches are commonly used for an accurate prediction of the forming behaviour, especially in order to optimise component and process design as well as to shorten development times. For this purpose, investigations of the yielding and fracture behaviour of magnesium alloys have to be performed in an adequate way. Even though, many publications thematising plastic behaviour of magnesium alloys already exist, the investigation of failure properties at elevated temperatures has not been adequately studied so far.

Conventionally forming limit curves (FLC) are used to describe the formability of sheet metal materials. The fracture behaviour of AZ31 by means of Nakajima-tests or FLC has been investigated in different studies yet [1, 2, 3]. Nevertheless, FLC are only valid for linear strain paths due to the current determination procedure. Furthermore, this procedure does not imply material testing for standardised shear dominated stress states and is not appropriate to predict shear fracture. Besides, some materials (like high-strength steel) tend to show fracture behaviour without prior localized necking. This also cannot be predicted with a FLC. Alternatively, stress state dependent fracture models can be used. Modern models of this kind, like Modified-Mohr-Coulomb (MMC), describe fracture initiation in dependence on stress triaxiality  $\eta$  and normalised Lode angle  $\bar{\theta}$  [4]. The stress triaxiality  $\eta$  is defined by:

$$\eta = \frac{\sigma_m}{\bar{\sigma}} \quad (1)$$

with the mean major stress  $\sigma_m$  and the equivalent stress  $\bar{\sigma}$ .

The normalised Lode angle  $\bar{\theta}$  is calculated based on the following correlation:

$$\bar{\theta} = 1 - \frac{2}{\pi} \arccos(\xi) \quad (2)$$

using the parameter of Lode angle  $\xi$ , which is defined with the major stresses  $\sigma_I$ ,  $\sigma_{II}$  and  $\sigma_{III}$  by:

$$\xi = \frac{27(\sigma_I - \sigma_m)(\sigma_{II} - \sigma_m)(\sigma_{III} - \sigma_m)}{2(1/2[(\sigma_I - \sigma_{II})^2 + (\sigma_{II} - \sigma_{III})^2 + (\sigma_I - \sigma_{III})^2])^{2/3}} \quad (3)$$

According to the MMC- model, the fracture strain  $\bar{\epsilon}_f$  can be described by five parameters including three material parameters  $C_1$ ,  $C_2$ ,  $C_3$  as well as  $A$  and  $n$  (the latter two from Swift hardening law) [5] as follows:

$$\bar{\epsilon}_f(\eta, \bar{\theta}) = \left\{ \frac{A}{C_2} \left[ C_3 + \frac{\sqrt{3}}{2-\sqrt{3}} (1 - C_3) \left( \sec\left(\frac{\bar{\theta}\pi}{6}\right) - 1 \right) \right] \cdot \left[ \sqrt{\frac{1+C_1^2}{3}} \cdot \cos\left(\frac{\bar{\theta}\pi}{6}\right) + C_1 \left( \eta + \frac{1}{3} \sin\left(\frac{\bar{\theta}\pi}{6}\right) \right) \right] \right\}^{-1/n} \quad (4)$$

With the definition of a damage variable  $D$ , the equivalent strain  $d\bar{\epsilon}$  is incrementally contributed to the damage accumulation in dependence of  $\bar{\epsilon}_f(\eta, \bar{\theta})$  [5] by following equation:

$$D = \int_0^{\bar{\epsilon}} \frac{d\bar{\epsilon}}{\bar{\epsilon}_f(\eta, \bar{\theta})} \quad (5)$$

It is assumed, that fracture initiates when  $D = 1$  ( $d\bar{\epsilon} = \bar{\epsilon}_f(\eta, \bar{\theta})$ ). On the basis of this, also non-linear strain-paths (or non-radial loading paths) are considered using such kind of model. The MMC- model achieved good results in validation studies predicting fracture in sheet metal forming processes with aluminium [5] and high strength steels [6, 7]. The calibration of stress state based fracture models is not standardized yet. A comprehensive study analysing pros and cons of different tests is presented in [8]. Studies investigating the fracture behaviour of magnesium sheet alloys

in order to parameterise stress state fracture models like the MMC- model are very rare in literature. Jia and Bai [9] performed a comprehensive set of mechanical tests under multiaxial loading conditions in order to characterise the plastic and fracture behaviour of AZ31, but only at room temperature. Sheet forming processes with magnesium alloys are limited by the low formability of magnesium alloys at room temperature due to their hexagonal close-packed crystal structure. Therefore, they are generally applied at elevated temperatures due to the enhanced formability of magnesium by an activation of non-basal slip systems. Thus, the description of fracture behaviour of magnesium sheet alloys should be focused on at elevated temperatures ( $> 200\text{ }^{\circ}\text{C}$ ). For this reason, in this study the fracture behavior of a magnesium sheet alloy was investigated at elevated temperatures. Therefore, a heated testing device with a recently developed new butterfly specimen and experimental-numerical approach was used in order to determine appropriate data for calibration of a stress-based fracture model.

### Nomenclature

$A$	Material parameter of Swift hardening law
$C_{1,2,3}$	Material parameter of MMC- model
$D$	Damage variable
FLC	Forming limit curve
MMC	Modified-Mohr- Coulomb
$n$	Material parameter of Swift hardening law
$\bar{\epsilon}$	Equivalent strain
$\bar{\epsilon}_f$	Fracture strain
$\eta$	Stress triaxiality
$\bar{\theta}$	Normalised Lode angle
$\xi$	Lode angle
$\bar{\sigma}$	Equivalent stress
$\sigma_{I,II,III}$	Major stresses
$\sigma_m$	Mean major stress

## 2. Experimental setup and procedure

The material under investigation is an AZ31 magnesium sheet alloy from POSCO manufactured by strip casting with a nominal thickness of 2.0 mm. In this study a recently developed butterfly specimen [11] was used in order to investigate the fracture behavior of the AZ31 magnesium alloy, see Fig. 1.

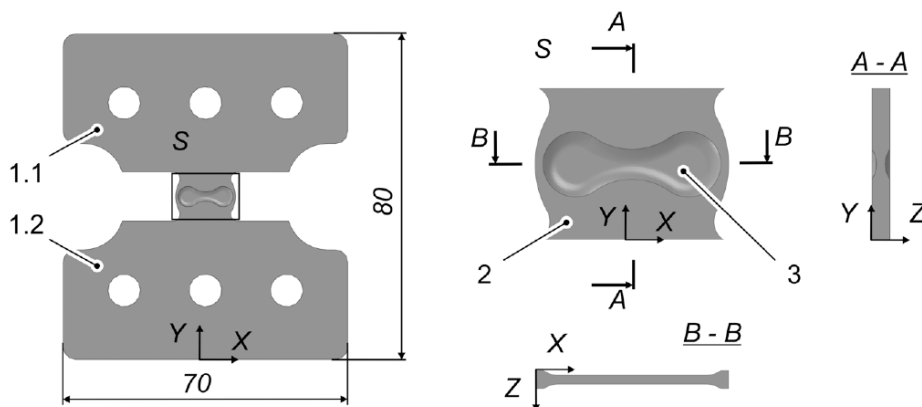


Fig. 1. Geometry of butterfly specimen [11].

The investigation area (Area 3 in Fig. 1) of the specimen has a special optimized geometry with a reduced thickness with 25% of the initial sheet thickness. The thickness reduction is carried out by means of machining, whereby the roughness values of  $R_a < 0.8$  and  $R_z < 6.3$  are ensured. The center of the specimen is similar to the one of Bai et al. [10]. Irrespective of the load application angle, the fracture initiates in the center of the investigation area at the desired stress state [11].

In order to perform tests on the butterfly specimen, a tool for uniaxial tensile testing machines shown in Fig. 2 was used. The tool consists of two fixtures, which are firmly attached to the pistons of the machine and have a slot to accommodate two half-disk shaped specimen holders. Due to the adjustable specimen holders, a desired specimen orientation relative to the test loading direction can be realised. Each of the fixtures and the corresponding specimen holders has seven holes through which pins are inserted to lock the specimen holders in a particular orientation and prevent them from rotating during the test. By this means, load application angles between  $-3^\circ$  and  $90^\circ$  with steps of  $15.5^\circ$  can be realised with the setup. In order to be able to run temperature-controlled tests, the holders were redesigned in two parts with integrated heating pipes. The heating temperature in the setup was monitored and controlled by thermocouples of type K. Therefore, a thermocouple was welded next to the investigation area of the specimen in each test to ensure a purposed temperature in the investigation area of the specimen. During the heating periods, care was taken to ensure that thermal expansion was compensated directly by the tensile machine in order to not affect the sample. The tests were carried out under quasi-static conditions with a velocity of 0.02 mm/s. During the tests, the investigation area of the specimen was continuously recorded by optical measurement system Aramis by (Fig. 2, right). Furthermore, the relative displacement of the specimen holders was optically recorded by reference points on the fastening plates close to the analysis area of the specimen. With the presented specimen and setup, tests in three application angles  $\alpha$  of  $-3^\circ$ ,  $28^\circ$  and  $59^\circ$  were performed (for definition of  $\alpha$ , see Fig. 3).

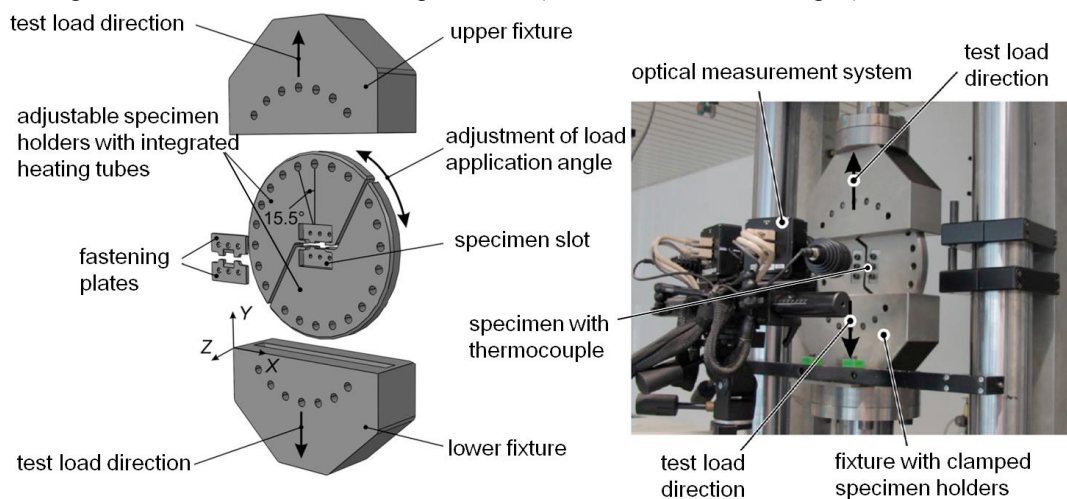


Fig. 2. Tool principle and setup for tests with the butterfly specimen at elevated temperatures.

### 3. Numerical approach

#### 3.1. FE-Model

Numerical simulations of the experimental tests of the previous section were carried out in order to determine strain and stress developments with which the location at fracture initiation can be characterised. Due to excessive shear deformation and temperature influence, the applied paint pattern in the investigation area of the specimen went corrupt and could not be evaluated. In Fig. 3, the used FE-model is schematically shown. A mesh size of 0.15 mm was used in the model. Experimentally identified relative displacements for the onset of fracture, which were obtained in the previous section, were set for the displacement  $u_{x,y}$  as boundary conditions in the FE-simulation.

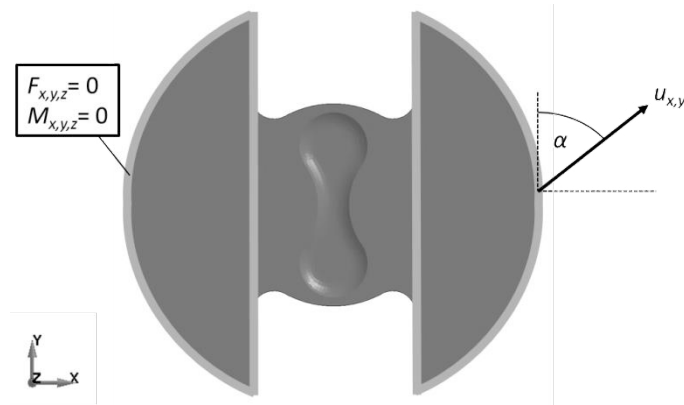


Fig.3. FE-Model of performed butterfly tests with boundary conditions.

### 3.2. Material model

Magnesium alloys exhibit an orthotropic yielding behaviour. Due to the loading case, different crystal twinning systems in the microstructure of the material are activated, called extension twins  $\{10\text{-}12\}\langle 10\text{-}1\text{-}1\rangle$  and contraction twins  $\{10\text{-}11\}\langle 10\text{-}1\text{-}2\rangle$  [12, 13] resulting in an asymmetric yielding behaviour between tensile and compressive loadings. It was shown exemplary in [14, 15] for room temperature and [16] for elevated temperatures that the specific yielding behaviour of magnesium alloys can be described with the yield criterion CPB06, which was developed by Cazacu, Plunkett, Barlat [17]. In order to parameterise the CPB06 yield criterion for the particular AZ31 magnesium alloy, which is used in this study, an approach by performing tensile, compressive and biaxial tests has been already presented by the authors in [16]. The parameters of CPB06 were implemented in the material model MAT\_233 of LS-Dyna. At elevated temperatures, magnesium alloys exhibit hardening deterioration (softening) associated with dynamic recovery and dynamic re-crystallization [15]. The softening behaviour beyond the uniform deformation limit has been characterised by an experimental extrapolation of yield curves by means of sheet layer compression tests [16]. For this purpose, the method from Sigvant et al. [18] for the transformation of a biaxial yielding curve into an uniaxial stress state was used as described in [19, 20]. In Fig. 4, the combined yield curves for the two investigated temperatures 180 °C and 230 °C are depicted. The results are approximately consistent with those from [21], which were determined by inverse numerical calibration for an AZ31 sheet alloy.

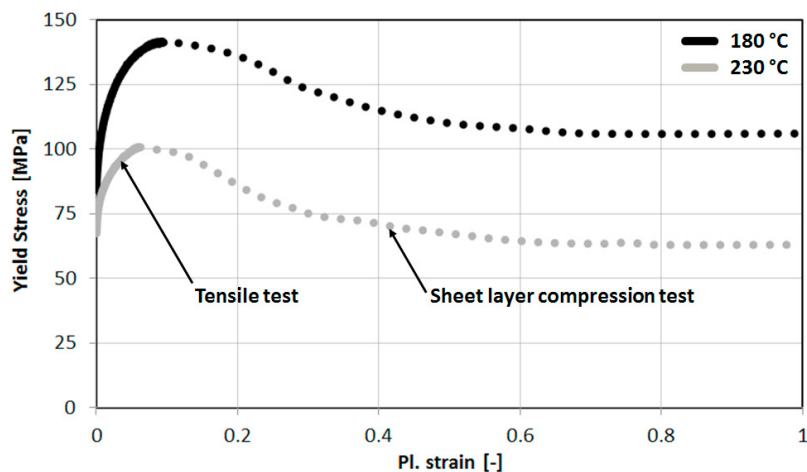


Fig. 4. Yield curves from tensile and sheet layer compression tests for 180 °C and 230 °C.

### 4. Experimental and numerical results

In performed tests, fracture initiation occurred in the desired zone in the middle of the investigation area, what is exemplarily depicted in Fig. 5 for two different loading angles at 180 °C. In the dependence of the load application angle, two different characteristic fracture modes could be distinguished, what is shown in the depicted micro sections (Fig. 5, right). For an angle of  $\alpha = -3^\circ$ , typical brittle or shear fracture occurred; ductile fracture type was observed for  $\alpha = 59^\circ$ . The MMC- model can be used for both fracture types. The onset of fracture was detected by observing the appearance of the first crack with the optical measurement system.

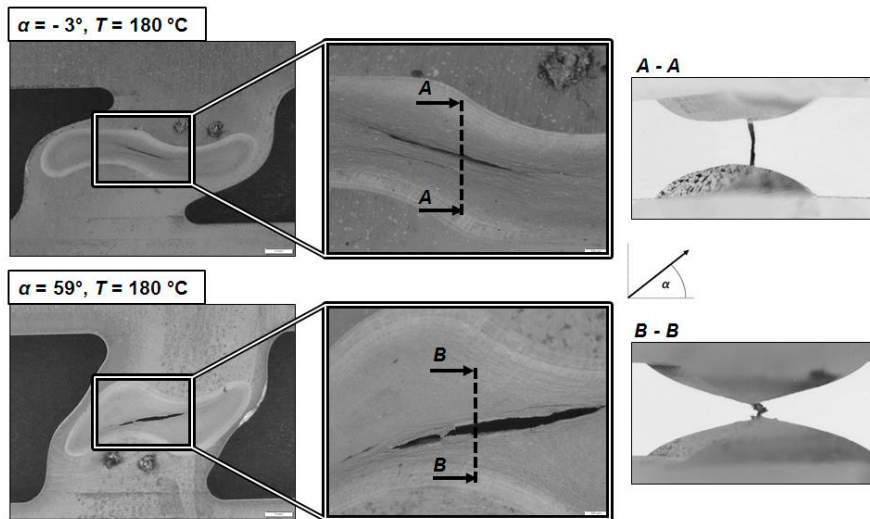


Fig. 5. Experimental results for load application angles  $-3^\circ$  and  $59^\circ$ , forming temperature 180 °C.

In Fig. 6, the experimental and numerical force-displacement developments for the butterfly tests are compared. It can be seen that the used material model achieved satisfactory results for different load application angles or stress states and the two investigated temperatures.

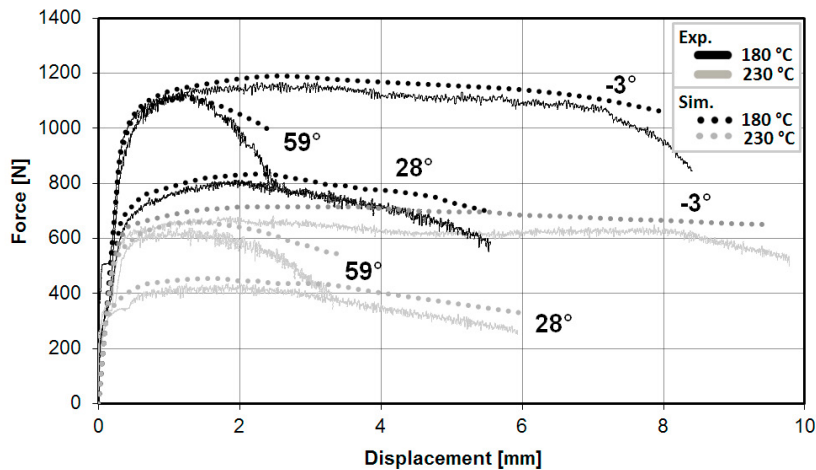


Fig. 6. Force-displacement developments for butterfly tests with load application angles  $\alpha$  of  $-3^\circ$ ,  $28^\circ$  and  $59^\circ$  for investigated temperatures (180 °C, 230°C).

For the determination of characteristic strain and stress values, elements exhibiting the highest strain (in the center of the investigation area) were evaluated from the simulations. Thereby, forming stages for experimentally determined fracture displacements were considered. By this means, the triaxiality and Lode angle developments were determined for each load application angle  $\alpha$ . On the basis of a weighted mean, a specific triaxiality value was determined for each test. Subsequently, equation 4 was used to parameterise the damage model. The parameterised fracture curves for the MMC- model are depicted in Fig. 7 for a plane stress condition. The parameters of the MMC-model can be found in Table 1. Finally, the fracture curve can be implemented in most FE-programs (e. g. LS-Dyna, Abaqus) in order to estimate damage evolution during forming processes with AZ31.

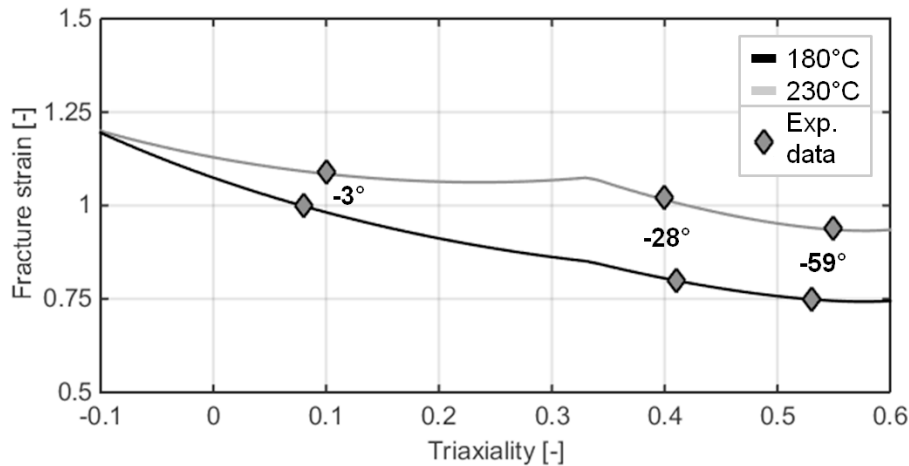


Fig. 7. Fracture curve (plane stress,  $\bar{\theta} = 0$ ) for the MMC- model (AZ31, 180 °C and 230 °C).

Table 1. Determined parameter of the MMC- model.

Temperature	$C_1$	$C_2$	$C_3$	$A$	$n$
180 °C	0.081	0.197	1.022	191.1	0.121
230 °C	0.035	0.140	1.025	134.6	0.103

## 5. Conclusion

A test setup for butterfly-tests at elevated temperatures was presented. By means of the setup, different stress states can be tested with one specimen geometry by variation of the load application angle. A characterisation of the fracture behaviour of an AZ31 magnesium sheet alloy was performed by aid of numerical stress evaluation. For this purpose, an orthotropic yielding criterion CPB06 combined with characterised softening behaviour was used to obtain prospering results. By means of the numerical-experimental investigation, specific parameters for calibration of stress state models were gained and finally a MMC- model was parameterised for forming temperatures at 180 °C and 230 °C. The study proved applicability of the new setup for tests with butterfly specimen in order to characterise the fracture behaviour of AZ31 magnesium sheet at elevated temperatures in dependence of the stress state.

## Acknowledgments

The authors are much obliged to the DFG (Deutsche Forschungsgemeinschaft, German Research Foundation) for the financial support of project 44192561.

## References

- [1] Bruni, C.; Forcellese, A.; Gabrielli, F.; Simoncini, M. (2010): Effect of temperature, strain rate and fibre orientation on the plastic flow behaviour and formability of AZ31 magnesium alloy. In *Journal of Materials Processing Technology* 210 (10), pp. 1354–1363.
- [2] Stutz, L.; Bohlen, J.; Kurz, G.; Letzig, D.; Kainer, K. U. (2011): Influence of the Processing of Magnesium Alloys AZ31 and ZE10 on the Sheet Formability at Elevated Temperature. In *KEM* 473, pp. 335–342.
- [3] Forcellese, A.; El Mehtedi, M.; Simoncini, M.; Spigarelli, S. (2007): Formability and Microstructure of AZ31 Magnesium Alloy Sheets. In *KEM* 344, pp. 31–38.
- [4] Bai, Y.; Wierzbicki, T. (2008): A new model of metal plasticity and fracture with pressure and Lode dependence. In *International Journal of Plasticity* 24 (6), pp. 1071–1096.
- [5] Beese, A. M.; Luo, M.; Li, Y.; Bai, Y.; Wierzbicki, T. (2010): Partially coupled anisotropic fracture model for aluminum sheets. In: *Engineering Fracture Mechanics* 77 (7), pp. 1128–1152.
- [6] Li, Y.; Luo, M.; Gerlach, J.; Wierzbicki, T. (2010): Prediction of shear-induced fracture in sheet metal forming. In: *Journal of Materials Processing Technology* 210 (14), S. 1858–1869.
- [7] Behrens, B-A; Bonk, C.; Peshekhodov, I. (2017): On modelling of shear fracture in deep drawing of a high-strength dual-phase sheet steel. *Journal of Physics: Conference Series* 896, p. 12125.
- [8] Peshekhodov, I.; Dykiert, M.; Vucetic, M.; Behrens, B-A (2016): Evaluation of common tests for fracture characterisation of advanced high-strength sheet steels with the help of the FEA. In *IOP Conf. Ser.: Mater. Sci. Eng.* 159, p. 12014.
- [9] Y. Jia; Y. Bai (2016): Experimental study on the mechanical properties of AZ31B-H24 magnesium alloy sheets under various loading conditions, *International Journal of Fracture* 197,1 pp. 25–48.
- [10] Bai, Y.; Wierzbicki, T. (2008): A new model of metal plasticity and fracture with pressure and Lode dependence, *International Journal of Plasticity* 24 (6), pp. 1071–1096.
- [11] Peshekhodov, I.; Jiang, S.; Vucetic, M.; Bouguecha, A.; Berhens, B-A (2016): Experimental-numerical evaluation of a new butterfly specimen for fracture characterisation of AHSS in a wide range of stress states. In *IOP Conference Series: Materials Science and Engineering* 159, p. 12015.
- [12] Lou, X.; Li, M.; Boger, R.; Agnew, S.; Wagoner, R. (2007): Hardening evolution of AZ31B Mg sheet, In *International Journal of Plasticity* 23 (1), pp. 44-86.
- [13] Dudamell, N. V.; Ulacia, I.; Gálvez, F.; Yi, S.; Bohlen, J.; Letzig, D. et al. (2012): Influence of texture on the recrystallization mechanisms in an AZ31 Mg sheet alloy at dynamic rates. In *Materials Science and Engineering: A* 532, pp. 528-535.
- [14] Chandola, N.; Lebensohn R. A.; Cazacu, O.; Revil-Baudard, B.; Mishra R. K.; Barlat, F. (2015): Combined effects of anisotropy and tension-compression asymmetry on the torsional response of 5AZ316 Mg. In *International Journal of Solids and Structures* 58, pp. 190-200.
- [15] Andar, M. O.; Kuwabara, T.; Steglich, D. (2012): Material modeling of AZ31 Mg sheet considering variation of r-values and asymmetry of the yield locus. In *Materials Science and Engineering: A* 549, pp. 82-92.
- [16] Behrens, B.-A.; Bouguecha, A.; Bonk, C.; Dykiert, M. (2017): Experimental Characterization and Material Modelling of an AZ31 Magnesium Sheet Alloy at Elevated Temperatures under Consideration of the Tension-Compression Asymmetry. In: *Journal of Physics: Conference Series* 896 (1), p. 12019.
- [17] Cazacu, Oana; Plunkett, Brian; Barlat, Frédéric (2006): Orthotropic yield criterion for hexagonal closed packed metals. In *International Journal of Plasticity* 22 (7), pp. 1171-1194.
- [18] Sigvant, M., Mattiasson, K., Vegter, H. et al. (2009) *Int J Mater Form* 2: 235.
- [19] Behrens, B.-A.; Bouguecha, A.; Huinink, T.; Peshekhodov, I.; Matthias, T.; Moritz, J.; Schrödter, J. (2013): Investigation of the flow behavior of wrought magnesium alloy AZ31 using layer compression and tensile tests. In *Mat.-wiss. u. Werkstofftech.* 44 (9), pp. 760-767.
- [20] Behrens, B.-A.; Bouguecha, A.; Vucetic, M.; Peshekhodov, I. (2012): Characterisation of the quasi-static flow and fracture behaviour of dual-phase steel sheets in a wide range of plane stress states. In *Archives of Civil and Mechanical Engineering* 12 (4), pp. 397–406.
- [21] Lee, C.; Koh, Y.; Seok, D.-Y.; Kim, H.; Lee, M.-G.; Chung, K. (2016): Mechanical property of magnesium alloy sheet with hardening deterioration at warm temperatures and its application for failure analysis. Part II – failure analysis. In *Int J Mater Form* 9 (3), pp. 287–295.